

Influence of the Linear Aromatic Density on Methylene Blue Aggregation around Polyanions Containing Sulfonate Groups

Ignacio Moreno-Villoslada,^{*,†} César Torres-Gallegos,[†] Rodrigo Araya-Hermosilla,[†] and Hiroyuki Nishide[‡]

Instituto de Química, Facultad de Ciencias, Universidad Austral de Chile, Casilla 567, Valdivia, Chile, and Department of Applied Chemistry, School of Science and Engineering, Waseda University, Tokyo 169-8555, Japan

Received: September 21, 2009; Revised Manuscript Received: February 1, 2010

The aggregation of methylene blue around different polyelectrolytes is studied by diafiltration, UV–vis, and ¹H NMR spectroscopies. Poly(sodium acrylate-*co*-sodium maleate) induces the formation of higher-order aggregates, showing a typical polyelectrolyte behavior dominated by long-range electrostatic interactions with the dye which are highly dependent on the ionic strength. Poly(sodium 4-styrenesulfonate) presents a high dispersant ability of methylene blue, showing what we can call a typical polyaromatic-anion behavior characterized by the presence of short-range aromatic–aromatic interactions with the dye which are less dependent on the ionic strength. An intermediate behavior is found for the copolymers poly(sodium 4-styrenesulfonate-*co*-sodium maleate) at two different comonomer compositions, related to a different probability of the polymers to form and stabilize ion pairs in hydrophobic environments. Their behavior is a function of the linear aromatic density, which is related to the comonomeric structure.

1. Introduction

The standard theory regarding the interactions between polyelectrolytes and their counterions is based on long-range electrostatic interactions, and described by the counterion condensation theory of G. S. Manning.^{1–4} According to Manning's theory, a higher concentration of hydrated counterions is found around the polymer chains; these counterions are able to move on the polymer surface, so that the interaction is considered non-site-specific. Long-range electrostatic interactions may be considered primary interactions between polyelectrolytes and their counterions. However, when additional secondary interactions such as hydrogen bonding, coordination binding, or aromatic–aromatic interactions are held, the general picture for the polyelectrolyte–counterion interaction may change dramatically. By means of these secondary interactions, supramolecular assemblies based on charged molecules can be achieved with controlled structure and geometry, and nanoscale architectures with different functionalities may be designed under the so-called ionic self-assembly (ISA).^{5–22} ISA is usually accompanied by a cooperative binding mechanism,^{23,24} by means of which the molecules bind preferably adjacent to each other: the first bonds stimulate further binding which propagates toward the final self-assembled structures. The cooperativity of the ionic binding process is of major importance in ISA, and the reason for the simplicity of synthesis, structural perfection, and stability of related nanoassemblies.

Among secondary interactions, short-range aromatic–aromatic interactions^{25–28} arise as an important tool to control the structure and properties of supramolecular assemblies. They are one of the principal noncovalent forces governing molecular recognition and biomolecular structure. They are important in the stabiliza-

tion of DNA and its association with intercalators.^{28–31} They also play an important role in protein stabilization^{32–35} and protein functionality, as in enzymes,^{36,37} transmembrane channels,^{38,39} etc. The major contribution to aromatic–aromatic interactions arises from van der Waals interactions, including solvophobic effects, while short-range electrostatic interactions determine the geometry of the interaction.²⁶

Charged dye molecules are excellent building blocks for supramolecular chemistry and may show a defined and regular shape for mutual overlap interactions due to aromatic–aromatic interactions. The cooperative binding of charged dyes on polyelectrolytes is already a classic theme and has been used in polyelectrolyte analytics.^{9,18–22,40–47} This is the case of porphyrins^{9,41–45} and xanthene dyes such as rhodamine B⁴⁶ and methylene blue (MB).^{40,47} Depending on their concentration, two mechanisms can be described to understand the behavior of nonaromatic polyelectrolyte–dye association. For diluted solutions, monomeric dyes bind the polyelectrolyte due to long-range interactions that produce non-site-specific binding, and, providing a higher local concentration of dyes on their environment, the dyes self-aggregate on the surface of the polyelectrolytes. For concentrated solutions of the dye, dye aggregates may interact as a whole with the polyelectrolyte, so that the dye aggregates may behave as supramolecular polyelectrolytes and interpolymer complexes may be described.

On the other hand, we have recently described that polyelectrolytes containing aromatic rings may undergo short-range aromatic–aromatic interactions with aromatic counterions. These interactions are particularly strong when the polyelectrolyte charge is supported on the polymeric aromatic ring, and may constitute the major forces driving the interaction with the counterions.^{46–54} We point out as relevant the dispersant ability of polymers such as poly(sodium 4-styrenesulfonate) (PSS) for counterions such as xanthenes dyes,^{46,47} or poly(4-vinylpyridine) for counterions such as sulfonated porphyrins,⁵⁴ as well as the resistance of the interaction to the cleaving effect of added NaCl.

* To whom correspondence should be addressed. Fax: 56-63-293520. E-mail: imorenovilloslada@uach.cl.

[†] Universidad Austral de Chile.

[‡] Waseda University.

These findings can open new possibilities for the formation of nanostructures under the scope of ISA. By means of these short-range interactions, site-specific binding between the counterion and the polymeric aromatic functional groups is held, and hydrophobic ion pairs are formed; these ion pairs tend to aggregate depending on the polyelectrolyte/counterion ratio, a fact that may be crucial for the behavior, structure, and properties of the systems. Under appropriate conditions, the self-stacking tendency of aromatic counterions such as charged dyes may be overcome: in the presence of a moderate excess of polymeric functional groups (typically 10 times), ion pairs aggregate, but in the presence of a high excess of the polymer (typically 100 times), ion pairs are far from each other and do not aggregate. Thus, these polyelectrolytes may inhibit the cooperative binding tendency of the counterions, showing a certain dispersant ability. The dispersant ability of aromatic polyelectrolytes may be of potential use in controlling counterion properties and may serve to monitor the importance of secondary aromatic–aromatic interactions between the polyelectrolyte and the counterions. Other systems described in the literature involving the interaction between polyelectrolytes and aromatic counterions reveal the different behavior considering the presence or the lack of aromaticity on the polyelectrolytes.^{9,12,55}

Of particular interest was the finding that the linear aromatic density of polyelectrolytes containing benzenesulfonate moieties, defined as the amount of aromatic groups per length unit of the polymer chain, affected the binding ability of 2,3,5-triphenyl-2*H*-tetrazolium chloride to the polyanions and the protection from reduction with ascorbic acid that these polymers furnished.^{52,53}

Apart from spectroscopic techniques, separation techniques such as diafiltration (DF) are useful to evaluate the binding between polyelectrolytes and low molecular-weight species (LMWS).^{56–63} The main magnitudes managed in DF analyses are the filtration factor (F), defined as the ratio between the volume in the filtrate and the constant volume in the DF cell, the concentration in the filtrate of the LMWS under study ($c_{\text{LMWS}}^{\text{filtrate}}$), the concentration of free LMWS in the cell solution ($c_{\text{LMWS}}^{\text{free}}$), the concentration of LMWS reversibly bound to the polyelectrolyte ($c_{\text{LMWS}}^{\text{rev-bound}}$), the apparent dissociation constant ($K_{\text{LMWS}}^{\text{diss}}$), defined as the ratio $c_{\text{LMWS}}^{\text{free}}/c_{\text{LMWS}}^{\text{rev-bound}}$, the DF parameters k^m , j , u , and v , and the polymer concentration in mole per liter of monomeric units (c_p). k^m and j parameters (the absolute value of the slope of the curve $\ln c_{\text{LMWS}}^{\text{filtrate}}$ versus F in the absence and in the presence of the polyelectrolyte, respectively) are related to the strength of the interaction, while v and u are related to the amounts of LMWS reversibly or irreversibly bound to the polymer, respectively. By irreversibly bound we consider molecules bound in processes that may be reversible with an apparent dissociation constant that tend to zero at the conditions of the experiment.

The aim of this paper is to discuss differences in the mode of binding of MB to polyelectrolytes with different linear aromatic density such as PSS, poly(sodium 4-styrenesulfonate-*co*-sodium maleate) at comonomer compositions 3:1 (P(SS₃-*co*-MA₁)) and 1:1 (P(SS₁-*co*-MA₁)), and poly(sodium acrylate-*co*-sodium maleate) at a comonomer composition 1:1 (P(AA₁-*co*-MA₁)). ¹H NMR and UV–vis spectroscopies are used to evaluate these interactions, as well as DF.

2. Experimental Section

2.1. Reagents. Commercially available PSS (Aldrich, synthesized from the para-substituted monomer), P(SS₃-*co*-MA₁) (Aldrich), P(SS₁-*co*-MA₁) (Aldrich), P(AA₁-*co*-MA₁) (Aldrich),

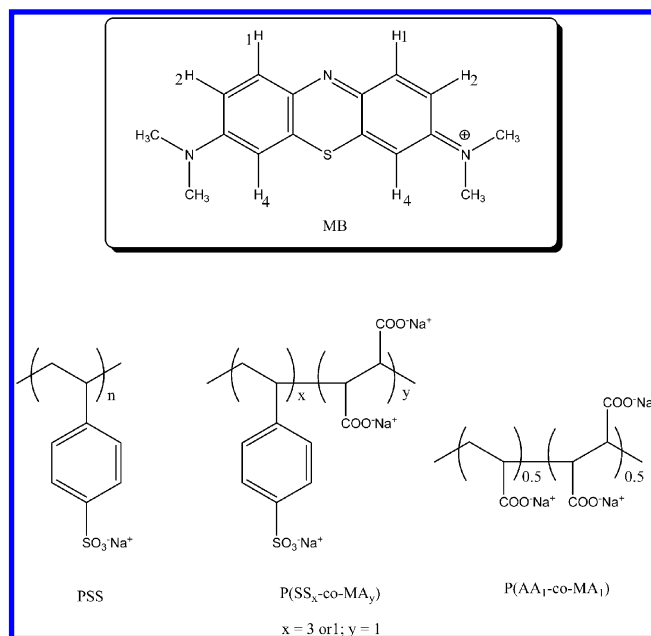


Figure 1. Molecular structures.

and MB (Synth) were used to prepare the solutions in deionized distilled water. The structures of the different polyelectrolytes and MB are shown in Figure 1. The pH was adjusted with NaOH and HCl. NaCl (Scharlau) was used to adjust the ionic strength.

2.2. Equipment. The unit used for DF studies consisted of a filtration cell (Amicon 8010, 10 mL capacity) with a magnetic stirrer, a regenerated cellulose membrane with a molecular-weight cutoff of 5000 Da (Ultracel PLCC, 25 mm diameter), a reservoir, a selector, and a pressure source. Distilled water was deionized in a Simplicity Millipore deionizer. The pH was controlled on a Hanna pH211 or Horiba F-15 pH meters. UV–vis measurements were performed in a Helios γ spectrophotometer. ¹H NMR measurements were made in a JNM-Lambda500 (JEOL, 500 MHz) spectrometer.

2.3. Procedures. Conventional and well-known procedures have been followed for DF, ¹H NMR, and UV–vis. Particular experimental conditions are provided in the figure captions. Details for DF procedures can be found elsewhere.^{61–63} Prior to use, the polyelectrolytes were fractionated over a polyether-sulfone membrane with a molecular-weight cutoff of 10 000 Da, and the highest molecular-weight fractions were chosen for DF experiments in order that no macromolecule is able to traverse the 5000 Da DF membrane. ¹H NMR experiments were done in D₂O at 298 K. UV–vis measurements were recorded using optical path lengths ranging between 1.0 and 10^{−2} cm for solutions containing MB at concentrations between 10^{−5} and 10^{−3} M, in order to have absorbances in the range 0.1–1.0. The pH was adjusted to 7 in all experiments. The polymer concentration is given in mole of sulfonate (or acrylate) units per liter in all experiments.

3. Results and Discussion

3.1. Different Polyelectrolytes. In this work, the concentration of the polymers is given in mole of sulfonate units per liter (acrylate units per liter in the case of P(AA₁-*co*-MA₁)), and, in order to compare between the different polyelectrolytes, the same concentration is kept in a series of experiments. That makes certain that the presence of maleate moieties in the copolymers bearing sulfonate groups can be regarded as the inclusion of additional charges on the polyelectrolyte chains,

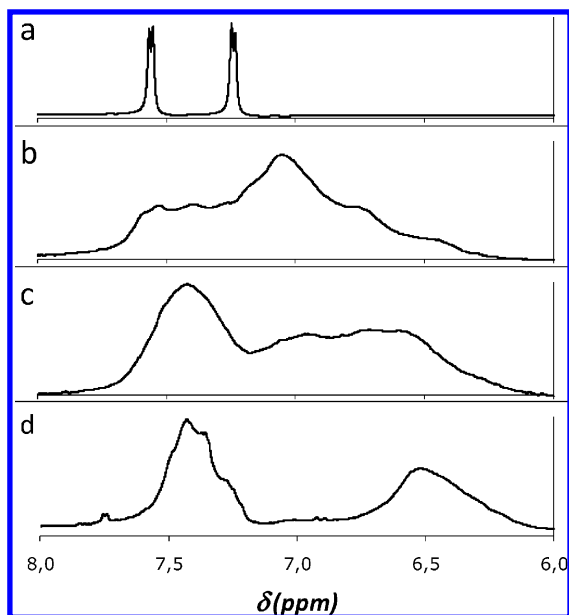


Figure 2. 500 MHz ^1H NMR spectra of 10^{-2} M of (a) sodium *p*-toluenesulfonate; (b) P(SS₁-co-MA₁); (c) P(SS₃-co-MA₁); and (d) PSS.

taking PSS as reference. Due to the tendency of maleic acid derivatives to produce alternate copolymers, it can be assumed that the maleate units are inserted between two styrenesulfonate residues. Thus, the linear aromatic density of the copolymers decreases as the number of maleate units increases. Besides, it can be considered that the hydrophilicity of the copolymers increases as the linear aromatic density decreases, which may produce more extended conformations on the copolymers. Differences in the ^1H NMR spectra of the aromatic region concerning the different polyelectrolytes are found despite the fact that they bear the same aromatic functional groups, as can be seen in Figure 2. In order to have a reference for comparison, the spectrum of sodium *p*-toluenesulfonate is also represented, where it can be seen that the signals of both groups of equivalent protons appear at 7.57 and 7.23 ppm. As the linear aromatic density of the polymers increases, signals appear consecutively upfield shifted up to 6.5 ppm. An explanation for this is the higher probability of the aromatic groups to stack on each other by means of aromatic–aromatic interactions, so that the magnetic fields produced by close rings affect the ^1H resonances.^{47,48,64}

3.2. Self-Stacking of MB in Water. MB undergoes self-aggregation in water by increasing its concentration, as is widely recognized.^{65–67} As a consequence of this, an increase in the intensity of the band at around 610 nm in UV–vis spectroscopy with respect to the band centered at 666 nm is observed, due to an increase in the probability to produce H-type contacts, as can be seen in Figure 3. The band centered around 610 nm is commonly associated with dimerization, while the band centered at 666 nm corresponds to monomeric MB. The presence of added electrolytes enhances the self-aggregation of the dye, and in the presence of 0.1 M NaCl, the ratio between the dimer band (610 nm) versus the monomer band (666 nm) increases.

This self-aggregation can also be observed by ^1H NMR since aromatic–aromatic interactions between dye molecules are responsible for the H-type contacts, so that the flat aromatic MB molecules stack on each other. When aromatic rings stack on each other, one aromatic ring places in the shielding cone of the other, resulting in upfield shifts of ^1H resonances. Upfield shifts of the aromatic signals of MB are observed as their concentration increases, as can be seen in Figure 4. This effect

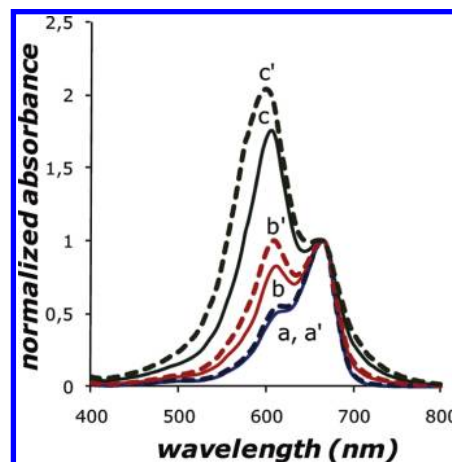


Figure 3. Normalized UV–vis spectra of MB in the absence (a,b,c) and in the presence of 0.1 M NaCl (a',b',c') at concentrations 10^{-5} M (a,a'), 10^{-4} M (b,b'), and 10^{-3} M (c,c').

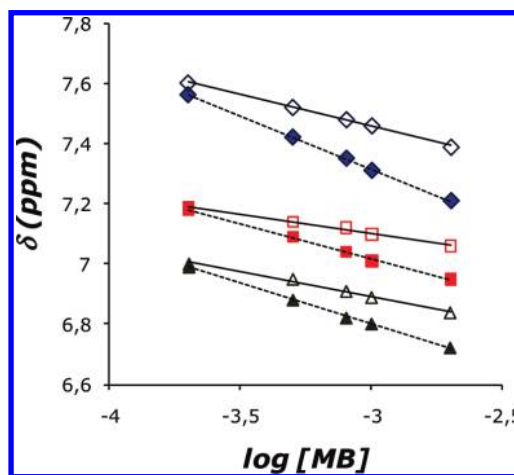


Figure 4. Chemical shifts (δ) of MB aromatic protons as a function of the logarithm of MB concentration in the absence (empty symbols) and in the presence of 0.1 M NaCl (filled symbols). H1 (\diamond , \blacklozenge), H2 (\square , \blacksquare), and H4 (\triangle , \blacktriangle).

is more noticeable in the presence of 0.1 M NaCl. At MB concentration of 2×10^{-4} M the effect of the salt is practically negligible. However, at a concentration of 2×10^{-3} M the difference in the chemical shifts of the aromatic MB signals reach values between 0.1 and 0.2 ppm, indicating a higher occurrence of H-contacts in the presence of the salt. The different chemical shifts are a linear function of the logarithm of the MB concentration, with a higher absolute value of the slope in the presence of 0.1 M NaCl as can be seen in Figure 4.

3.3. Self-Stacking of MB in the Presence of P(AA₁-co-MA₁). Self-aggregation of MB in the form of large aggregates on negatively charged surfaces such as zeolites,⁶⁸ silica,⁶⁹ dendrimers,⁷⁰ and polyelectrolytes^{40,47} is described in the literature and revealed by a shift to higher energies of the absorbance band in UV–vis experiments. This self-aggregation is due to secondary aromatic–aromatic interactions induced by a higher local concentration of the dye around the different objects, which provide with charge compensation. The binding of MB to negatively charged polyelectrolytes has been shown to be cooperative.^{40,47} A similar behavior has been found for the interaction of MB with P(AA₁-co-MA₁). In the presence of this polyelectrolyte, higher-order aggregates are formed, which are clearly seen in Figure 5 by the appearance of a band at around 570 nm in UV–vis spectroscopy. In ^1H NMR spectroscopy,

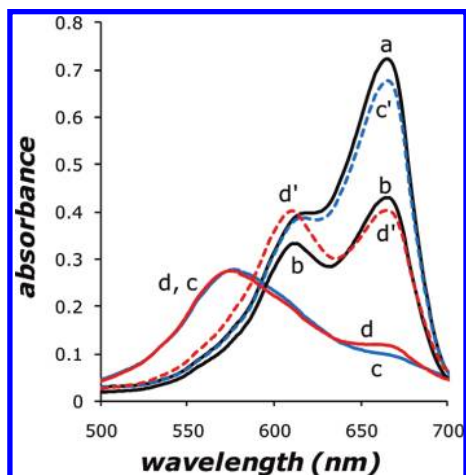


Figure 5. UV-vis spectra of (a) 10^{-5} M MB in the absence of any additive; (b) 10^{-4} M MB in the absence of any additive; (c) 10^{-5} M MB in the presence of 10^{-4} M P(AA₁-co-MA₁); (c') 10^{-5} M MB in the presence of 10^{-4} M P(AA₁-co-MA₁) and 0.1 M NaCl; (d) 10^{-4} M MB in the presence of 10^{-3} M P(AA₁-co-MA₁); and (d') 10^{-4} M MB in the presence of 10^{-3} M P(AA₁-co-MA₁) and 0.1 M NaCl.

copy, the formation of higher-order aggregates produces upfield shifts of the aromatic signals between 0.4 and 0.7 ppm with respect to the signals found in the absence of the polymer, as can be seen in Figure 6a. Note that in the presence of the polyelectrolyte there is not a high dependence of the chemical shifts on the MB concentration as the polymer is 10 times in excess over the dye. Long-range electrostatic interactions are easily cleaved in the presence of added electrolytes in excess as NaCl. It can be seen in Figure 5 that the band of monomeric MB is recuperated in the presence of 0.1 M NaCl for diluted solutions (10^{-5} M), indicating the cleaving of the self-aggregation due to the electrostatic shielding between the dye and the polyelectrolyte. For higher concentrations of MB (10^{-4} M), the self-aggregation of MB is minimized in the presence of 0.1 M NaCl, although the polymer still slightly enhances it (spectrum d' in Figure 5) with respect to the self-aggregation found in the absence of the polymer (spectrum b in Figure 5). The ^1H NMR upfield shifts are also minimized at MB concentrations in the range of the sensibility of the technique, as can be seen in Figure 6b, although residual self-aggregation is also detected when comparing the situation in the absence of the polymer.

In summary, P(AA₁-co-MA₁) presents a typical polyelectrolyte behavior characterized by the presence of long-range

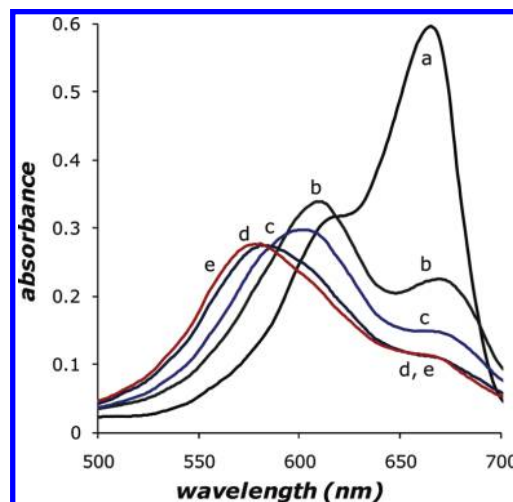


Figure 7. UV-vis spectra of 10^{-5} M MB: (a) in the absence of any polyelectrolyte; (b) in the presence of 10^{-4} M PSS; (c) in the presence of 10^{-4} M P(SS₃-co-MA₁); (d) in the presence of 10^{-4} M P(SS₃-co-MA₁); and (e) in the presence of 10^{-4} M P(AA₁-co-MA₁).

electrostatic interactions with MB, a high dependence of the interaction on the ionic strength, and the ability to induce higher-order aggregates, thus presenting a low dispersant ability of the dye.

3.4. Binding of MB to PSS. The binding of MB to the polyanion PSS is governed by short-range aromatic-aromatic interactions.⁴⁷ This is a consequence of a combination of hydrophobic forces, short-range electrostatic interactions between the aromatic groups, and short-range electrostatic interactions between the net positive and negative charges that MB and PSS respectively bear. Site-specific binding of the dye molecules to the polymeric benzenesulfonate moieties is held. This changes the behavior of this system in comparison to typical polyelectrolytes. Ion pairs are formed, and these ion pairs tend to aggregate, this tendency being a function of the polymer/dye ratio. Thus, under a moderate excess of the polyelectrolyte (10 times), the dye molecules are dispersed randomly distributed on the polymeric binding sites, so that self-aggregation in the form of large aggregates is minimized. Comparing to the situation with P(AA₁-co-MA₁), this is reflected in UV-vis experiments by a decrease of the intensity of the band at around 570 nm, the appearance of an intense dimer band at around 610 nm, and an increase on the monomer band, as can be seen in Figure 7. The high intensity of the dimer band is due to ion

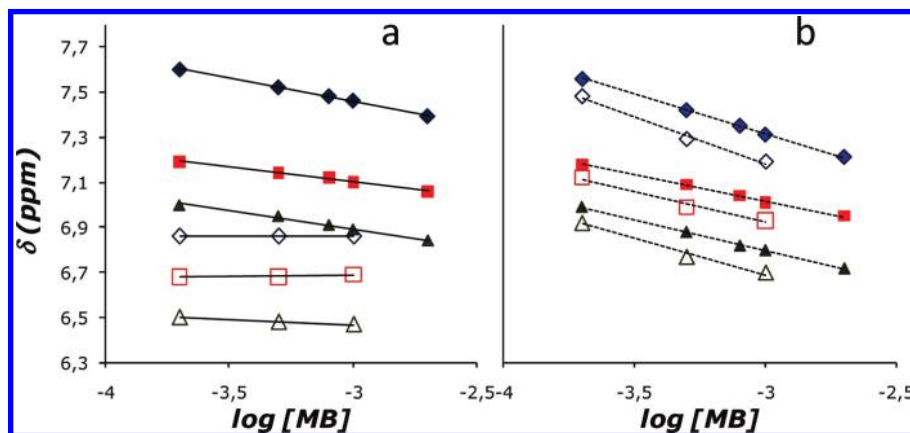


Figure 6. Chemical shifts (δ) of MB aromatic protons as a function of the logarithm of MB concentration in the absence of any polyelectrolyte (filled symbols) and in the presence of 10 times P(AA₁-co-MA₁) (empty symbols); and in the absence (a, left) and in the presence of 0.1 M NaCl (b, right): H1 (\diamond , \blacklozenge), H2 (\square , \blacksquare), and H4 (\triangle , \blacktriangle).

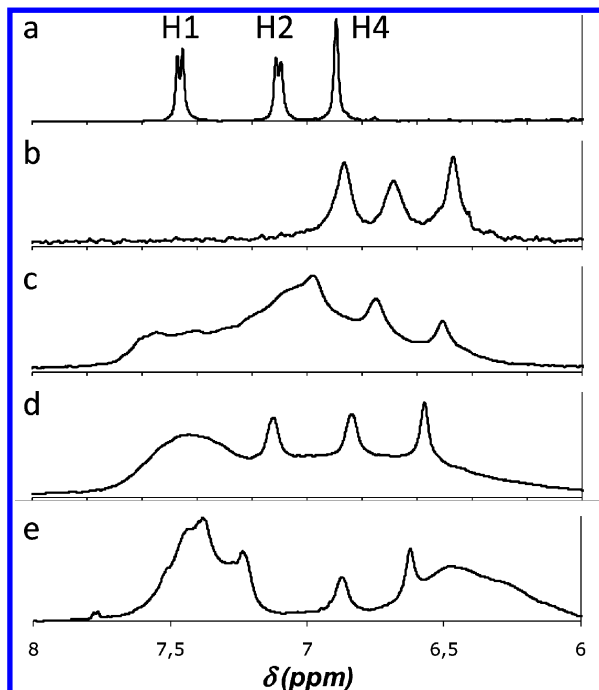


Figure 8. 500 MHz ^1H NMR spectra of 10^{-3} M MB in the absence of any polyelectrolyte (a) and in the presence of 10^{-2} M of P(AA₁-co-MA₁) (b); P(SS₁-co-MA₁) (c); P(SS₃-co-MA₁) (d); and PSS (e).

pair aggregation, and the intensity decreases for higher relative polymer concentrations.⁴⁷

Examples in the literature concerning PSS brushes⁹ and porphyrins showed a similar behavior. Under a moderate excess of benzenesulfonate groups (from 1 to 10 times) a band at 418 nm appears. This band is shifted 6 nm to lower energies with respect to the band corresponding to free monomeric porphyrins (412 nm). According to our interpretation, and contrasted in similar systems,^{46,47,54,55} this band should correspond to monomeric porphyrins stacked on the benzenesulfonate groups. The shift of the monomer band to lower energies is attributed to the interaction of the transition moment of the dyes with the surrounded molecules due to the short-range interaction.

The ^1H NMR spectra show MB bands broadened (Figure 8) and upfield shifted between 0.1 and 0.4 ppm in the presence of PSS with respect to the signals found in the absence of the polymer, as can be seen in Figures 8 and 9a, due to the influence of the magnetic fields produced by the stacked aromatic groups.

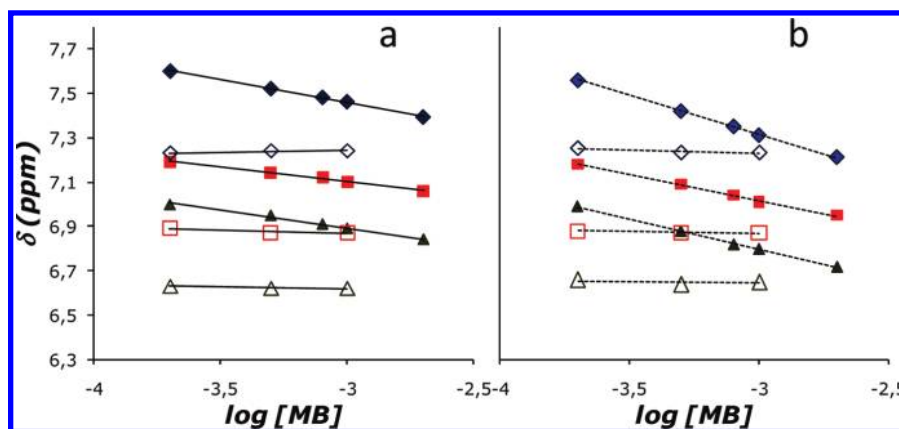


Figure 9. Chemical shifts (δ) of MB aromatic protons as a function of the logarithm of MB concentration in the absence of any polyelectrolyte (filled symbols) and in the presence of 10 times PSS (empty symbols); and in the absence (a, left) and in the presence of 0.1 M NaCl (b, right): H1 (\diamond , \blacklozenge), H2 (\square , \blacksquare), and H4 (\triangle , \blacktriangle).

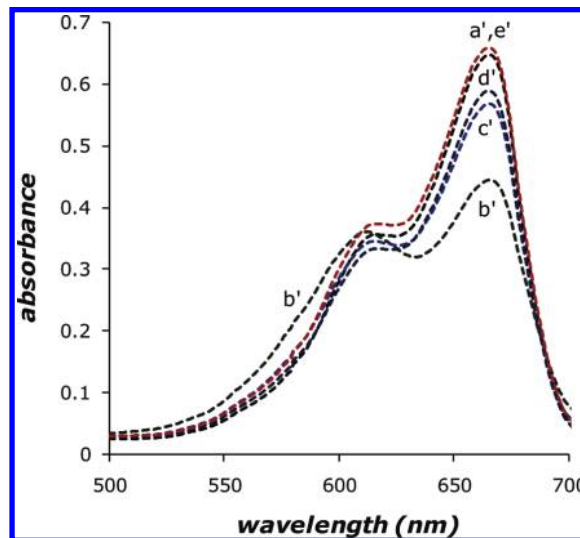


Figure 10. UV-vis spectra of 10^{-5} M MB in the presence of 0.1 M NaCl: (a') in the absence of any polyelectrolyte; (b') in the presence of 10^{-4} M PSS; (c') in the presence of 10^{-4} M P(SS₃-co-MA₁); (d') in the presence of 10^{-4} M P(SS₃-co-MA₁); and (e') in the presence of 10^{-4} M P(AA₁-co-MA₁).

Note that these upfield shifts are lower than in the case of P(AA₁-co-MA₁), indicating a different stacking mechanism. Since the most important parameter determining the MB environment is the relative polymer/MB concentration, the dye concentration does not affect the chemical shifts observed in Figure 9. On the other hand, as short-range aromatic-aromatic interactions are resistant to the cleaving effect of added electrolytes, the addition of NaCl does not affect much both UV-vis and ^1H NMR spectra: at the diluted concentrations used in UV-vis experiments (Figure 10), the dye aggregation is only partially cleaved, as seen by the presence of an intense dimer band and a monomer band less intense than for the free molecule, while ^1H NMR signals of more concentrated solutions do not change their position (Figure 9b).

In summary, PSS represents what we can call a typical polyaromatic-anion behavior characterized by the presence of short-range aromatic-aromatic interactions with MB, a low dependence of the interaction on the ionic strength, and a high dispersant ability of the dye.

3.5. Binding of MB in the Presence of Other Polyelectrolytes Bearing Benzenesulfonate Groups. In the two previous sections we have shown two different behaviors for two

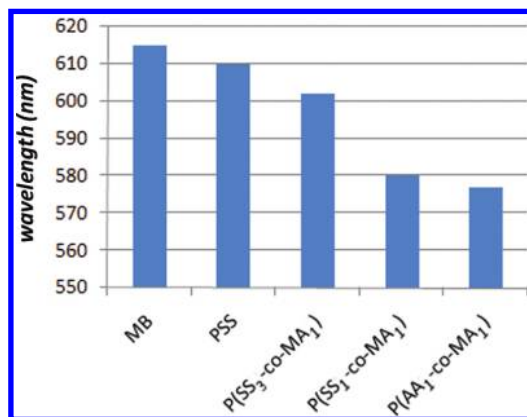


Figure 11. Position of the maximum of absorbance (nm) of the band corresponding to MB aggregates for a 10^{-5} M MB solution in the absence of any polyelectrolyte (MB) and in the presence of 10 times the different polyelectrolytes.

different polyelectrolytes that we can consider as reference for the analysis of other polyelectrolytes containing similar functional groups but different linear aromatic density. Experiments show that the copolymers P(SS₃-co-MA₁) and P(SS₁-co-MA₁) have an intermediate behavior.

The formation of higher order aggregates increases in the order PSS < P(SS₃-co-MA₁) < P(SS₁-co-MA₁) < P(AA₁-co-MA₁), showing an increasingly typical polyelectrolyte behavior. This can be seen in Figure 7: the band centered at around 570 nm in the case of P(AA₁-co-MA₁) shifts to lower energies as the linear aromatic density increases, indicating the formation of lower-order aggregates. The position of the maximum of absorbance corresponding to the band found at higher energies is shown in Figure 11 for every system. This change is accompanied by an increase on the intensity of the monomer band, revealing an increasing dispersant ability for the polyelectrolytes.

The addition of 0.1 M NaCl affects the aggregation state of the dye in the same order, as can be seen in Figure 10. Under these conditions, the long-range electrostatic component of the overall interaction between the polyelectrolytes and MB is cleaved, while the short-range aromatic–aromatic interaction between the benzenesulfonate rings and the dye may still be noticed. Large aggregates are quenched, leaving only monomers, isolated ion pairs, and, according to our interpretation, stacked ion pairs responsible for the more intense dimer band that appears in the polyelectrolytes with the highest aromatic density at the expense of the monomer band. The different ratio between the dimer and the monomer bands (D/M) found for the different polyelectrolytes is shown in Figure 12. As the linear aromatic density increases, this magnitude increases, showing the decrease on the cleaving effect of added NaCl. Thus, higher aggregation is found under these conditions when the linear aromatic density increases, due to the increasing importance of secondary aromatic–aromatic interactions between the dye and the polymer. This is attributed to a higher probability of ion pair aggregation, caused by differences in flexibility and hydrophilicity, and/or a different binding of the dye to the polyelectrolytes, and consequent different extent of ion pair formation.

In order to elucidate if the lack of aggregation is related to a lack of binding of MB to the polyelectrolytes, DF experiments have been done. Since DF is a separation technique, the apparent dissociation constants for the polyelectrolyte/dye complexes may be obtained. DF results throw quantitative binding for all systems in the absence of NaCl, and different and measurable

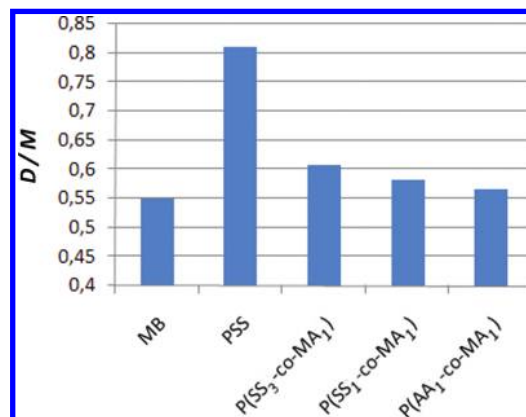


Figure 12. Ratio between the intensities of the dimer and monomer bands (D/M) for a 10^{-5} M MB solution in the absence of any polyelectrolyte (MB) and in the presence of 10 times the different polyelectrolytes.

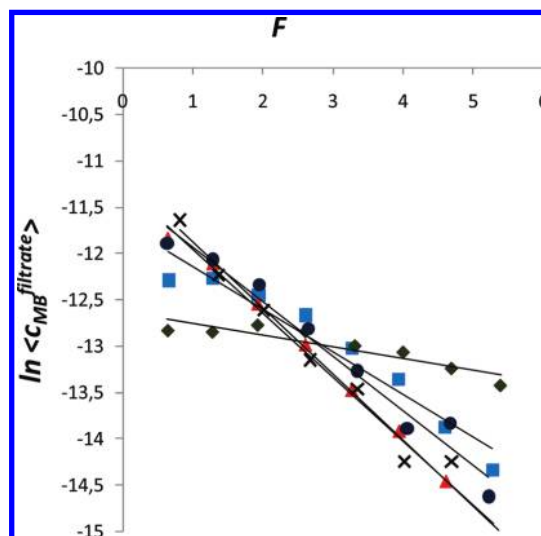


Figure 13. DF profiles of 2×10^{-5} M MB in the presence of 0.1 M NaCl: in the absence of any polyelectrolyte (\times) and in the presence of 2×10^{-4} M of P(AA₁-co-MA₁) (\blacktriangle), P(SS₁-co-MA₁) (\bullet), P(SS₃-co-MA₁) (\blacksquare), and PSS (\blacklozenge); expressions for the linear adjustments are found in Table 1.

K_{MB}^{diss} for diluted MB solutions in the presence of 0.1 M NaCl under a moderate excess of the polyelectrolytes. It can be seen in Figure 13 and Table 1 that the binding ability of the polyelectrolytes decreases as the linear aromatic density decreases, since lower slopes for the diafiltration profiles are found in the order PSS > PSS₃-co-MA₁ > PSS₁-co-MA₁ > PAA₁-co-MA₁, which correspond to K_{MB}^{diss} ranging between 0.15 and 2.5 for the polyelectrolytes containing aromatic groups. As the amount of aromatic moieties is the same for all the systems containing benzenesulfonate groups, it may signal the importance of the linear aromatic density on the strength of the aromatic–aromatic interaction between MB and the polymeric benzenesulfonate groups and on the consequent stabilization of the ion pairs formed, probably due to a higher hydrophobicity and/or a higher probability to undergo multiple stacking.

The shifting of the signals in ¹H NMR spectroscopy also correlates with the linear aromatic density, as can be seen in Figures 8 and 14. As the linear aromatic density decreases, the chemical shifts of the aromatic protons are increasingly upfield shifted, revealing a higher degree of aggregation, so that the polymers show lower dispersion ability, corresponding to an increasingly typical polyelectrolyte behavior. In the presence

TABLE 1: Results for DF of 2×10^{-5} M MB Solutions in the Presence of 0.1 M NaCl and Different Polyelectrolytes

expt	c_p (M)	ν	u	j	k^m	K_{MB}^{dissb}	linear adjustments for the exptl data ^a	R^2
MB–NaCl	—	0.9	0.1	—	0.71	—	$y = -0.71 \times -11.2$	0.98
PSS–MB–NaCl	2×10^{-4}	—	—	0.13	—	0.15 ± 0.04	$y = -0.13 \times -12.6$	0.83
P(SS ₃ -co-MA ₁)–MB–NaCl	2×10^{-4}	0.9	0.1	0.46	—	1.08 ± 0.42	$y = -0.46 \times -11.1$	0.94
P(SS ₁ -co-MA ₁)–MB–NaCl	2×10^{-4}	0.9	0.1	0.59	—	2.46 ± 1.48	$y = -0.59 \times -11.3$	0.97
P(AA ₁ -co-MA ₁)–MB–NaCl	2×10^{-4}	0.8	0.2	0.69	—	$\rightarrow \infty$	$y = -0.69 \times -11.3$	0.99

^a For linear adjustments: $y = \ln(c_{MB}^{filtrate})$; $x = F$; R^2 = linear regression factor. ^b K_{MB}^{diss} are calculated following $j/(1-j) \leq K_{MB}^{diss} \leq (k^m/j)/(k^m-j)$.

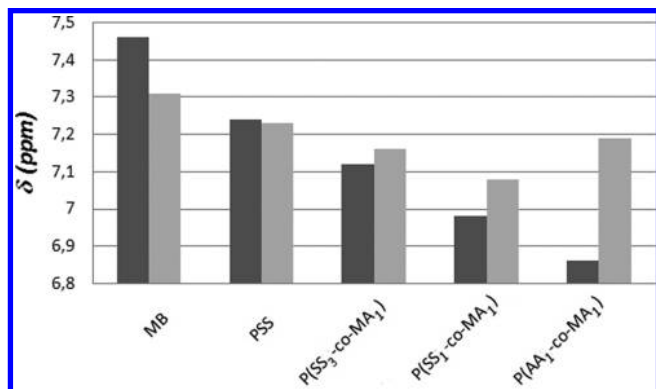


Figure 14. Chemical shifts (δ) of H1 in a 10^{-3} M MB solution in the absence (dark gray) and in the presence of 0.1 M NaCl (clear gray) obtained in the absence (MB) and in the presence of 10 times the different polyelectrolytes.

of NaCl, partial cleaving of the interaction at this high MB concentration increasingly takes place as the linear aromatic density decreases, resulting in lower upfield shifting of the signals, so that the differences between the chemical shifts in the presence and in the absence of salt increase. This fact is nearly negligible in the case of PSS and is more notorious in the case of the polyelectrolyte that does not contain aromatic groups.

3.6. Different Binding. Intermediate behavior between a typical polyelectrolyte behavior and a typical polyaromatic-anion behavior is found for the copolymers, related to a different probability of the polymers to form and stabilize ion pairs in hydrophobic environments. This is a function of the linear aromatic density, which is related to the comonomeric structure. A model to represent these observations is shown in Figure 15. Hydrophobic pockets have been represented, and their amount is not related to the number of benzenesulfonate groups, but to their density. As the number of hydrophobic pockets increases, the counterions are increasingly dispersed on the polymeric binding sites and their aggregation in the form of large aggregates due to their cooperative binding tendency is minimized. In the presence of NaCl, the resistance to the cleaving effect of the salt increases, so that the overall interaction increases.

4. Conclusions

P(AA₁-co-MA₁) presents a typical polyelectrolyte behavior characterized by the presence of long-range electrostatic interactions with MB, a high dependence of the interaction on the ionic strength, and the ability to induce higher-order aggregates, thus presenting a low dispersant ability of the dye. On the other hand, PSS represents what we can call a typical polyaromatic-anion behavior characterized by the presence of short-range aromatic–aromatic interactions with MB, a low dependence of the interaction on the ionic strength, and a high dispersant ability of the dye. The copolymers P(SS₃-co-MA₁) and P(SS₁-co-MA₁)

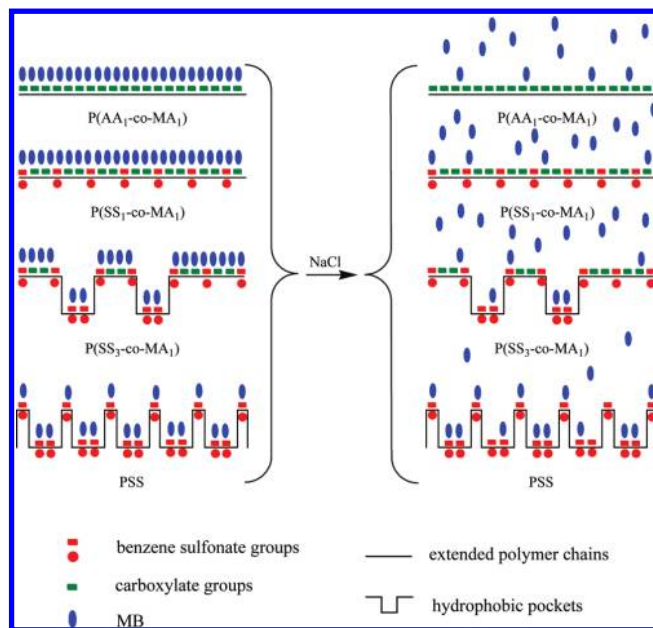


Figure 15. A graphical model of the binding of MB to the different polyelectrolytes in the presence and in the absence of NaCl.

present an intermediate behavior which is a function of their linear aromatic density. This is related to a different probability of the polymers to form and stabilize ion pairs in hydrophobic environments.

Acknowledgment. The authors thank Fondecyt (Grant No 1090341, Chile) and the Global COE program “Practical Chemical Wisdom” at Waseda University from MEXT, Japan, for financial support.

References and Notes

- (1) Manning, G. S. *Q. Rev. Biophys.* **1978**, *11*, 179.
- (2) Manning, G. S. *J. Phys. Chem.* **1984**, *88*, 6654.
- (3) Nordmeier, E. *Macromol. Chem. Phys.* **1995**, *196*, 1321.
- (4) Hao, M. H.; Harvey, S. C. *Macromolecules* **1992**, *25*, 2200.
- (5) Faul, C. F. J.; Antonietti, M. *Adv. Mater.* **2003**, *15*, 673.
- (6) Gröhn, F. *Macromol. Chem. Phys.* **2008**, *209*, 2295.
- (7) Willerich, I.; Gröhn, F. *Chem.—Eur. J.* **2008**, *14*, 9112.
- (8) Gröhn, F.; Klein, K.; Brand, S. *Chem.—Eur. J.* **2008**, *14*, 6866.
- (9) Ruthard, C.; Maskos, M.; Kolb, U.; Gröhn, F. *Macromolecules* **2009**, *42*, 830.
- (10) Yildiz, Ü.H.; Koynov, K.; Gröhn, F. *Macromol. Chem. Phys.* **2009**, *210*, 1678.
- (11) Kogej, K.; Evmenenko, G.; Theunissen, E.; Škerjanc, J.; Berghmans, H.; Reynaers, H.; Bras, W. *Macromol. Rapid Commun.* **2000**, *21*, 1226.
- (12) Kogej, K.; Evmenenko, G.; Theunissen, E.; Berghmans, H.; Reynaers, H. *Langmuir* **2001**, *17*, 3175.
- (13) Gohy, J. F.; Antoun, S.; Sobry, R.; van der Bossche, G.; Jerome, R. *Macromol. Chem. Phys.* **2000**, *201*, 31.
- (14) Thünemann, A. F.; Ruppelt, D.; Burger, C.; Müllen, K. *J. Mater. Chem.* **2000**, *10*, 1325.
- (15) De Santis, S.; Ladogana, D.; Diociaiuti, M.; Masci, G. *Macromolecules* **2010**, in press. DOI: 10.1021/ma9026542.
- (16) Antonietti, M.; Conrad, J.; Thünemann, A. *Macromolecules* **1994**, *27*, 6007.

- (17) Willerich, I.; Ritter, H.; Gröhn, F. *J. Phys. Chem. B* **2009**, *113*, 3339.
- (18) Würthner, F.; Thalacker, C.; Diele, S.; Tschierske, C. *Chem.—Eur. J.* **2001**, *7*, 2245.
- (19) Imae, T.; Gagel, L.; Tunich, C.; Platz, G.; Iwamoto, T.; Funayama, K. *Langmuir* **1998**, *14*, 2197.
- (20) Faul, C. F. J.; Antonietti, M. *Chem.—Eur. J.* **2002**, *8*, 2764.
- (21) von Berlepsch, H.; Böttcher, C.; Ouart, A.; Burger, C.; Dähne, S.; Kirstein, S. *J. Phys. Chem.* **2000**, *104*, 5255.
- (22) Horn, D. *Prog. Colloid Polym. Sci.* **1978**, *65*, 251.
- (23) Schwartz, G.; Klose, S.; Balthasar, W. *Eur. J. Biochem.* **1970**, *12*, 454.
- (24) Islam, Md. M.; Chowdhury, S. R.; Kumar, G. S. *J. Phys. Chem. B* **2009**, *113*, 1210.
- (25) Hunter, C. A.; Sanders, J. K. M. *J. Am. Chem. Soc.* **1990**, *112*, 5525.
- (26) Meyer, E. A.; Castellano, R. K.; Diederich, F. *Angew. Chem., Int. Ed.* **2003**, *42*, 1210.
- (27) Mignon, P.; Loverix, S.; De Proft, F.; Geerlings, P. *J. Phys. Chem. A* **2004**, *108*, 6038.
- (28) Mignon, P.; Loverix, S.; Steyaert, J.; Geerlings, P. *Nucleic Acids Res.* **2005**, *33*, 1779.
- (29) Marzilli, L. G.; Pethö, G.; Mengfen, L.; Kim, M. S.; Dixon, D. W. *J. Am. Chem. Soc.* **1992**, *114*, 7575.
- (30) McKnight, R. E.; Zhang, J.; Dixon, D. W. *Bioorg. Med. Chem. Lett.* **2004**, *14*, 401.
- (31) Martin, J. N.; Muñoz, E. M.; Schwergold, C.; Souard, F.; Asensio, J. L.; Jiménez-Barbero, J.; Cañada, J.; Vicent, C. *J. Am. Chem. Soc.* **2005**, *127*, 9518.
- (32) Tatko, Ch.D.; Waters, M. L. *Protein Sci.* **2003**, *12*, 2443.
- (33) Bodkin, M. J.; Goodfellow, J. M. *Protein Sci.* **1995**, *4*, 603.
- (34) Bhattacharyya, R.; Samanta, U.; Chakrabarti, P. *Protein Eng.* **2002**, *15*, 91.
- (35) Ranganathan, D.; Haridas, V.; Gilardi, R.; Karle, I. L. *J. Am. Chem. Soc.* **1998**, *120*, 10793.
- (36) Versées, W.; Loverix, S.; Vandemeulebroucke, A.; Geerlings, P.; Steyaert, J. *J. Mol. Biol.* **2004**, *338*, 1.
- (37) Greenblatt, H. M.; Dvir, H.; Silman, I.; Sussman, J. L. *J. Mol. Neurosci.* **2003**, *20*, 369.
- (38) Li, H. L.; Galue, A.; Meadows, L.; Ragsdale, D. S. *Mol. Pharmacol.* **1999**, *55*, 134.
- (39) Li, J.; Lester, H. A. *Chem.—Eur. J.* **2005**, *11*, 6525.
- (40) Soedjak, H. S. *Anal. Chem.* **1994**, *66*, 4514.
- (41) Egawa, Y.; Hayashida, R.; Anzai, J. *Langmuir* **2007**, *23*, 13146.
- (42) Kubát, P.; Lang, K.; Janda, P.; Anzenbacher, P. *Langmuir* **2005**, *21*, 9714.
- (43) Lauceri, R.; Campagna, T.; Raudino, A.; Purello, R. *Inorg. Chim. Acta* **2001**, *317*, 282.
- (44) Synytsya, A.; Synytsya, A.; Blafková, P.; Ederová, J.; Spěvaček, J.; Slepíčka, P.; Král, V.; Volka, K. *Biomacromolecules* **2009**, *10*, 1067.
- (45) Van Patten, P. G.; Shreve, A. P.; Donohoe, R. J. *J. Phys. Chem. B* **2000**, *104*, 5986.
- (46) Moreno-Villoslada, I.; González, F.; Arias, L.; Villatoro, J. M.; Ugarte, R.; Hess, S.; Nishide, H. *Dyes Pigments* **2009**, *82*, 401.
- (47) Moreno-Villoslada, I.; Torres, C.; González, F.; Nishide, H. *Macromol. Chem. Phys.* **2009**, *210*, 1167.
- (48) Moreno-Villoslada, I.; González, R.; Hess, S.; Rivas, B. L.; Shibuhe, T.; Nishide, H. *J. Phys. Chem. B* **2006**, *110*, 21576.
- (49) Moreno-Villoslada, I.; González, F.; Rivera, L.; Hess, S.; Rivas, B. L.; Shibuhe, T.; Nishide, H. *J. Phys. Chem. B* **2007**, *111*, 6146.
- (50) Moreno-Villoslada, I.; Jofré, M.; Miranda, V.; González, R.; Sotelo, T.; Hess, S.; Rivas, B. L. *J. Phys. Chem. B* **2006**, *110*, 11809.
- (51) Moreno-Villoslada, I.; González, F.; Rivas, B. L.; Shibuhe, T.; Nishide, H. *Polymer* **2007**, *48*, 799.
- (52) Moreno-Villoslada, I.; Soto, M.; González, F.; Hess, S.; Takemura, I.; Oyaizu, K.; Nishide, H. *J. Phys. Chem. B* **2008**, *112*, 5350.
- (53) Moreno-Villoslada, I.; González, F.; Soto, M.; Nishide, H. *J. Phys. Chem. B* **2008**, *112*, 11244.
- (54) Moreno-Villoslada, I.; Murakami, T.; Nishide, H. *Biomacromolecules* **2009**, *10*, 3341.
- (55) Zhao, L.; Ma, R.; Li, J.; Li, Y.; An, Y.; Shi, L. *Biomacromolecules* **2009**, *10*, 3343.
- (56) Geckeler, K. E.; Lange, G.; Eberhardt, H.; Bayer, E. *Pure Appl. Chem.* **1980**, *52*, 1883.
- (57) Uludag, Y.; Özbelge, H. Ö.; Yilmaz, L. *J. Membr. Sci.* **1997**, *129*, 93.
- (58) Juang, R.-S.; Liang, J.-F. *J. Membr. Sci.* **1993**, *82*, 163.
- (59) Rivas, B. L.; Moreno-Villoslada, I. *J. Phys. Chem. B* **1998**, *102*, 6994.
- (60) Rivas, B. L.; Moreno-Villoslada, I. *J. Phys. Chem. B* **1998**, *102*, 11024.
- (61) Rivas, B. L.; Pereira, E.; Moreno-Villoslada, I. *Prog. Polym. Sci.* **2003**, *28*, 173.
- (62) Moreno-Villoslada, I.; Miranda, V.; Oyarzún, F.; Hess, S.; Luna, M. B.; Rivas, B. L. *J. Chil. Chem. Soc.* **2004**, *49*, 121.
- (63) Moreno-Villoslada, I.; Miranda, V.; Chandía, P.; Villatoro, J. M.; Bulnes, J. L.; Cortés, M.; Hess, S.; Rivas, B. L. *J. Membr. Sci.* **2006**, *272*, 137.
- (64) Kim, J.; Raman, B.; Ahn, K. H. *J. Org. Chem.* **2006**, *71*, 38.
- (65) Michaelis, L.; Granick, S. *J. Am. Chem. Soc.* **1945**, *67*, 1212.
- (66) Spencer, W.; Sutter, J. R. *J. Phys. Chem.* **1979**, *83*, 1573.
- (67) Valdés-Aguilera, O.; Neckers, D. C. *Acc. Chem. Res.* **1989**, *22*, 171.
- (68) Ghanadzadeh, A.; Zanjanchi, M. A.; Tirbandpay, R. *J. Mol. Struct.* **2002**, *616*, 167.
- (69) Ohline, S. M.; Lee, S.; Williams, S.; Chang, C. *Chem. Phys. Lett.* **2001**, *346*, 9.
- (70) Jockusch, S.; Turro, N. J.; Tomaila, D. A. *Macromolecules* **1995**, *28*, 7416.